

RESEARCH ARTICLE

Open Access



# Analytical study of Buddha sculptures in Jingyin temple of Taiyuan, China

Xiaojian Bai<sup>1,3\*</sup> , Chen Jia<sup>2</sup>, Zhigen Chen<sup>2</sup>, Yuxuan Gong<sup>3</sup>, Huwei Cheng<sup>4</sup> and Jiayue Wang<sup>1</sup>

## Abstract

With exquisite design and unique style, the painted sculptures of Tutang Buddha and two attendants Buddha in Jingyin Temple are precious cultural heritages of China. The sculpture of Tutang Buddha, which was carved from a mound and painted by ancient craftsmen, was rarely found in ancient China. However, due to natural and human factors, the sculptures were severely damaged. Obviously, they require urgent and appropriate protection and restoration. In this study, samples taken from the sculptures were analysed through multiple analytical techniques, including scanning electron microscopy with energy dispersive spectrometry (SEM–EDS), Raman spectroscopy, X-ray diffraction (XRD), optical microscopy (OM) and granulometry. The analysis results enable us to infer the techniques used by the craftsmen in making the sculptures and provide a reliable evidence for the conservation and future protection of these and similar sculptures.

**Keywords:** Painted clay sculpture, Jingyin temple, Micro-raman, XRD, SEM–EDS, Granulometry, OM

## Introduction

Jingyin Temple, also known as Tutang Buddha Temple, is located in Tutang Village, 20 km northwest of Taiyuan, Shanxi Province, North China. It had been built during the Northern Qi dynasty, rebuilt in A.D. 1205 during the Jin dynasty and then partially restored during the Ming dynasty [1]. In addition, it had once been home to Fu Shan, an outstanding Taoist scholar and calligrapher, who lived in seclusion here for several times during the Ming and Qing dynasties [2]. In 2006, Jingyin Temple was declared a Key Cultural Relics Site under the State Protection. The Buddha Pavilion is the most important building in Jingyin Temple (Fig. 1a, b). The pavilion, which built on a cliff, is an east-facing two-story building with multiple eave hiped-roof. There are three painted sculptures in the hall of the Buddha Pavilion, where the Three Western Saints are worshiped [3]: Amitabha (Fig. 1c), Avolokitesvara (Fig. 1d) and Mahasthamaprapta (Fig. 1e).

The sculpture of Amitabha sitting on a raised platform, is one of the tallest Buddha sculptures in China that carved from earth mound and painted with natural pigments. Since it locates in Tutang Village, the sculpture is also known as “Tutang Buddha”. According to the earliest evidence of the origin of Tutang Buddha found in the inscriptions on the stone tablets [1], there was a hill piled with loess which suddenly collapsed into a cave. Inside the cave, a 33.3 m mound which was likely a Buddha was found. It was then sculpted into the Tutang Buddha, which is a bare-chested 9.46-m-tall Buddha wearing a robe and sitting on a 6-m-wide lotus seat with his hands in his lap. The sculpture was decorated with gold foils while the belt was painted with exquisite blue pattern (Fig. 2a). Its intricate patterns at the edge of the dress were drawn by the traditional Lifan technique (Fig. 2b). The Lifan technique, also called an embossed painting technique, is a high-level painting technique that was used widely in wall painting, sculpture and architectural painting in ancient China. According to the technique, the rubber powder is extruded by tools on the surface to form a 0.2-cm-high line, which highlights the three-dimensional sense of the pattern. Thus, these overall proved the preciousness of the sculpture [4].

\*Correspondence: baixiaojian@tyut.edu.cn

<sup>1</sup> Department of Cultural Heritage, Taiyuan University of Technology, Taiyuan 030024, China

Full list of author information is available at the end of the article



a



b



c

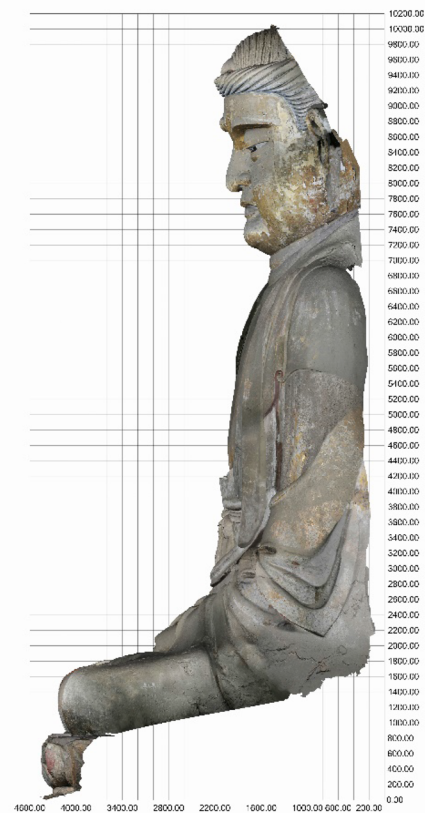
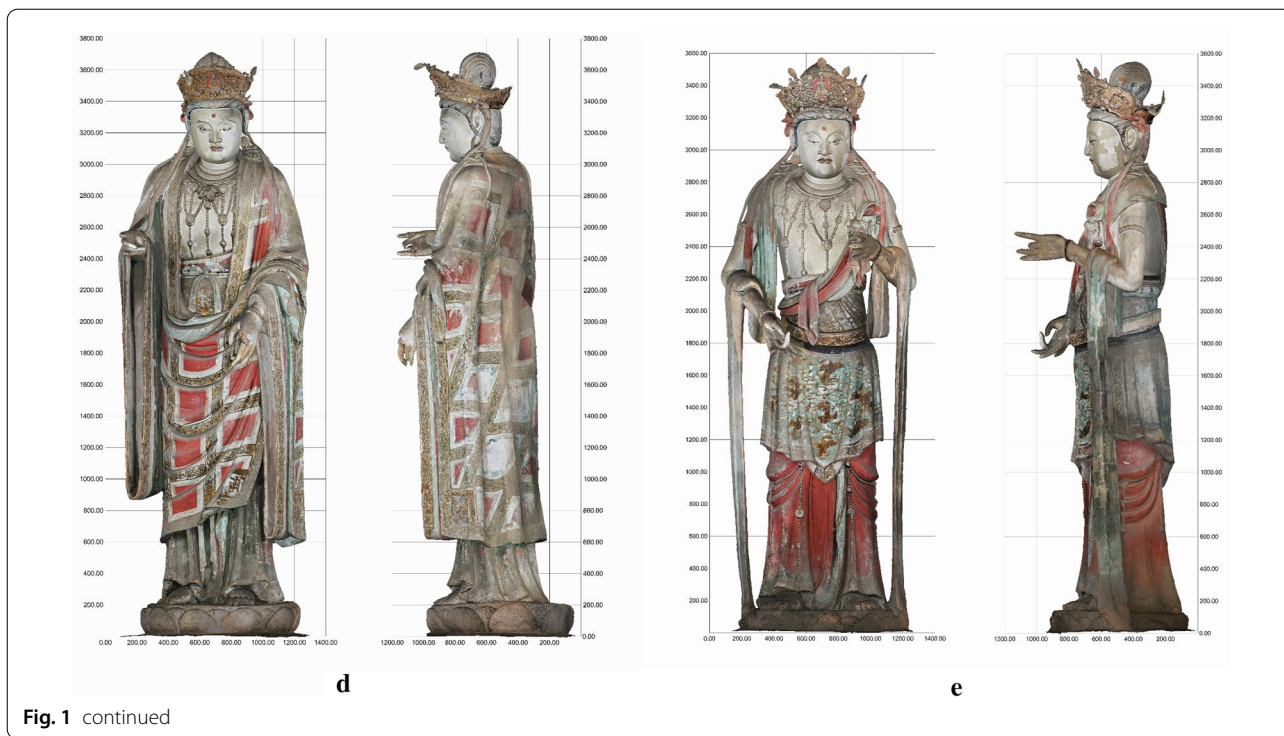


**Fig. 1** General view of the temple and the sculptures. **a** The interior of the Jingyin Temple; **b** The interior of the Buddha Pavilion; **c** Sculpture of Tutang Buddha; **d** Sculpture of Avalokitesvara bodhisattva; **e** Sculpture of Mahasthamaprapta bodhisattva (The cross-scale was marked in the unit of mm)



The sculptures of Avalokitesvara bodhisattva and Mahasthamaprapta bodhisattva are positioned face to face in a gentle and beautiful appearance. Both sculptures are 3.7 m tall, having pure white, broad, plump faces and wearing necklaces, bracelets and ornate clothes. References [1] showed that the two sculptures were made using the traditional sculpturing technology during the Ming dynasty as below [5]: the basic structure of the sculpture was built with wooden sticks of the mortise-tenon joint or fixed by nails; the wood skeleton was then wrapped with reed poles and fixed with hemp ropes; the cover consisted of coarse muds containing soil, sands and wheat straws, etc.; the thin layer was made of fine muds; the surface was whitened and painted. Complex patterning and gilding were applied onto the two sculptures to obtain the exquisite patterns.

Due to the natural and artificial deterioration, the sculptures were eroded severely, shown as flaking and shedding of the paint layer, salt corrosion, some damages found at the bottom of the sculptures, and detached and cracked fingers of the Avalokitesvara bodhisattva. Moreover, due to the pollutions such as surface dust and lampblack, the exquisite patterns became invisible. Thus, they require urgent preservation and restoration. In this respect, analytical studies become a reliable source for revealing the actual application of materials and the technique, as well as offering basic information for restoration.

Although studies on the sculptures have been conducted over the years [1, 2], only a few technical studies have been reported for the conservation of other sculptures and there is no previous technical investigation of the materials and techniques used in making the sculptures in Jingyin Temple. Considering all these modern methods, the combination of Environmental Scanning Electron Microscopy with Energy Dispersive X-ray analysis (ESEM/EDX), Raman spectroscopy and Polarized light microscopy (PLM) has proved to be a powerful methodology to identify the pigments [6–8]. Application of X-ray diffraction (XRD) is beneficial for accurately identifying crystalline structures in muds [9, 10]. Granulometric analysis is a well-established and powerful technique for analysing the particle sizes of caly samples [11]. The combination of Herzberg stain and optical microscope is used to distinguish the fiber sources, which is effective for identifying paper fiber [12]. In this work, micro-Raman spectroscopy, SEM–EDS, XRD, Granulometric analysis, OM were applied to analyse the fragments containing pigments, clay and paper. Such documentation and analysis not only offer basic information for the future conservation and restoration of the Temple, but also support the future study of the art history, age and ownership of the materials.

## Experimental

### Samples

Samples were taken from the damaged areas of the three painted sculptures, mainly the pigment, paper, and fine clay layers, following the procedures in accordance with *Principles for the Conservation of Heritage Sites in China* [13]. Since sampling refers to visible surfaces in the *Principles*, the coarse clay layers and wooden frames of the sculptures were not sampled. A small amount of undisturbed soil from the mountainside of the Juewei Mountain where Jingyin Temple is located was also sampled for comparison. The sample details are given in Table 1.

### Pigment identification

#### Digital microscopy

AM7915MZT Dino-Lite digital microscope was applied in in-situ observation of layers in the area of weak detail in order to examine the layer-structure and obtain the repainting information. The identifiable layers lay the basis for subsequent analytical studies carried out, explore technological details and provide useful information for screening protection and restoration methods.

#### Micro-Raman spectroscopy

Micro-Raman analysis of the pigment was performed using a XploRA Raman spectrometer (purchased from

Horiba Jobin–Yvon, France) coupled with an Olympus BX41 microscope. Point measurements were performed using an argon gas laser at 532 nm and a 50 × working distance objective. Measurements were performed in the LabSpec 5 acquisition software program at a spectral resolution of about 1 cm<sup>-1</sup>. Scanning times were determined for each sample separately, depending on the acceptable quality of the spectra obtained and also to ensure the samples were not altered due to the heating produced by the laser. In general, the scanning time varied between 10 and 60 s. The samples were measured over the spectrum range of 3000–100 cm<sup>-1</sup> with an accumulation number of 2. The spot size was 1 μm. The system used a 1200 groove/mm dispersive grating [14]. At least five measuring points were selected for each pigment.

#### Scanning electron microscopy with energy dispersive spectrometry (SEM–EDS)

SEM (a Quanta 650 of the FEI Company, USA) with EDS (a X-MaxN50 of the Oxford Instrument, UK.) were used for characterizing the elements of the pigment, which was a useful micro-destructive method for analysing samples of cultural relics. Each sample was put on the sample holder with conductive adhesive and gold sputtering technique was not used in the samples. Aztec software was used in the point & ID mode for micro-analysis. Samples were analysed with 20 kV acceleration voltage and 10 mm working distance.

#### Phase identification of clay minerals



##### X-ray diffractometer(XRD)

A rotating target X-ray diffractometer (Japan Makko Corporation MXPAHF 18 kW) equipped with a X-ray tube (Cu-Kα radiation: 1.541841 Å, 40 kV and 200 mA) was used to analyse the clay samples. The diffraction patterns were produced over the range of 10 to 70 degrees (2θ) with scanning speed was 8°/min and scanning step of 0.02.




#### Granulometry

Particle analysis of the clay samples was conducted. Plant fiber was removed from a sample by suspension and was heated to minimize its interference on particle size determination in the clay. The sample was then sonicated for 3 min to avoid sample reaggregation [11]. Laser particle size analyser was used to measure the ratio of total particle volume to total volume of all samples in a particular size range. BT-9300S laser granulometer was employed to

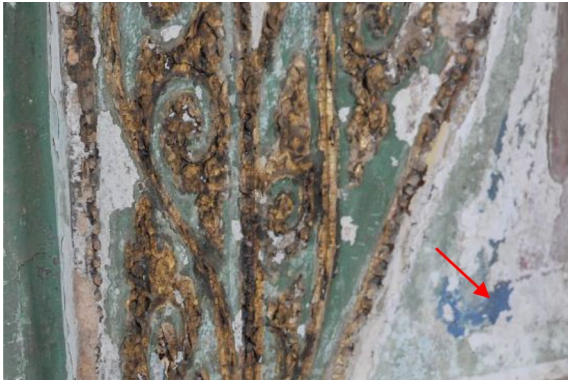
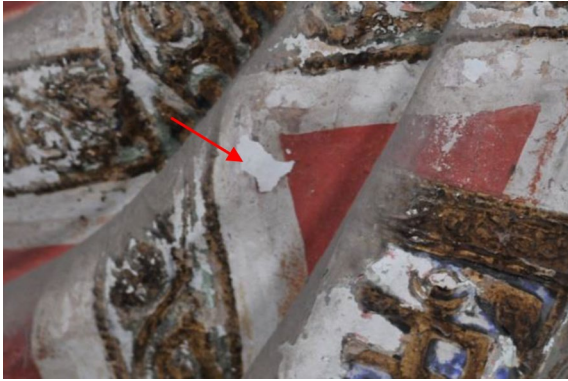
**Table 1 Details of samples**

Sample no	Sculpture	Photo of the sampling positions	Description
JYS-1-1	Tutang Buddha		Gold and paper in sublayer collected from lower part of the left side of Buddha
JYS-1-2	Tutang Buddha		Red pigment fragment collected from below the left sleeve of Buddha
JYS-1-3	Tutang Buddha		Red pigment fragment collected from lower part of the right side of Buddha
JYS-1-4	Tutang Buddha		White pigment fragment collected from lower part of the right side of Buddha

**Table 1 (continued)**

Sample no	Sculpture	Photo of the sampling positions	Description
JYS-1-5	Tutang Buddha		Fine clay layer fragment collected from the leg
JYS-1-6	Tutang Buddha		Black pigment fragment collected from the lower right part of Buddha
JYS-2-1	Avalokitesvara Bodhisattva		White pigment fragment collected from the right sleeve of sculpture

**Table 1 (continued)**

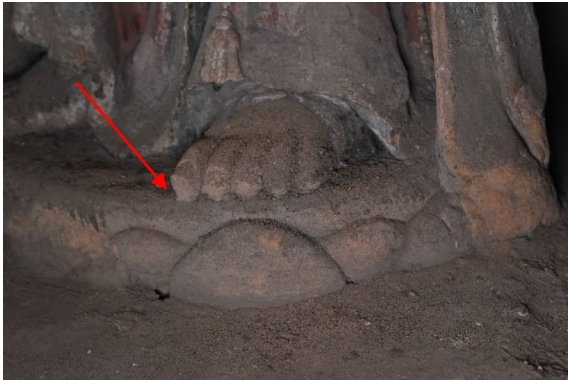

Sample no	Sculpture	Photo of the sampling positions	Description
JYS-2-2	Avalokitesvara Bodhisattva		Gold fragment collected from the left sleeve of sculpture
JYS-2-3	Avalokitesvara Bodhisattva		Red pigment fragment collected from Kasaya of the sculpture
JYS-2-4	Avalokitesvara Bodhisattva		Dark-blue pigment and paper in sublayer fragment collected from Kasaya of the sculpture
JYS-2-5	Avalokitesvara Bodhisattva		White pigment fragment collected from Kasaya of the sculpture

**Table 1 (continued)**

Sample no	Sculpture	Photo of the sampling positions	Description
JYS-2-6	Avalokitesvara Bodhisattva		Fine clay layer fragment collected from underneath the sculpture's feet
JYS-3-1	Mahasthamaprapta bodhisattva		Green pigment and paper in sublayer fragment collected from around the hemline of the left side of Buddha
JYS-3-2	Mahasthamaprapta bodhisattva		Gold fragment collected from the hemline of the left side of Buddha
JYS-3-3	Mahasthamaprapta bodhisattva		Black pigment fragment collected from the hemline of the left side of Buddha



**Table 1 (continued)**

Sample no	Sculpture	Photo of the sampling positions	Description
JYS-3-4	Mahasthamaprapta bodhisattva		Fine clay layer fragment collected from underneath the sculpture's feet
JYS-4	The mountainside		Mountain soil sample

measure the particle size ranging from 0.1 μm to 716 μm. The refractive index of the sample was set at 1.63.

**Fiber identification of paper**

**Optical microscopy (OM)**

Microscopic studies were performed on paper samples using a Leica DM2500 biological microscope for micro-morphology observation. Paper samples were immersed in water and dispersed into a single fiber. The fibers were placed on a glass slide and dyed with I<sub>2</sub>-ZnCl<sub>2</sub> solution. The biological microscope was used to observe fiber morphology and identify the specimen of the fiber [15].

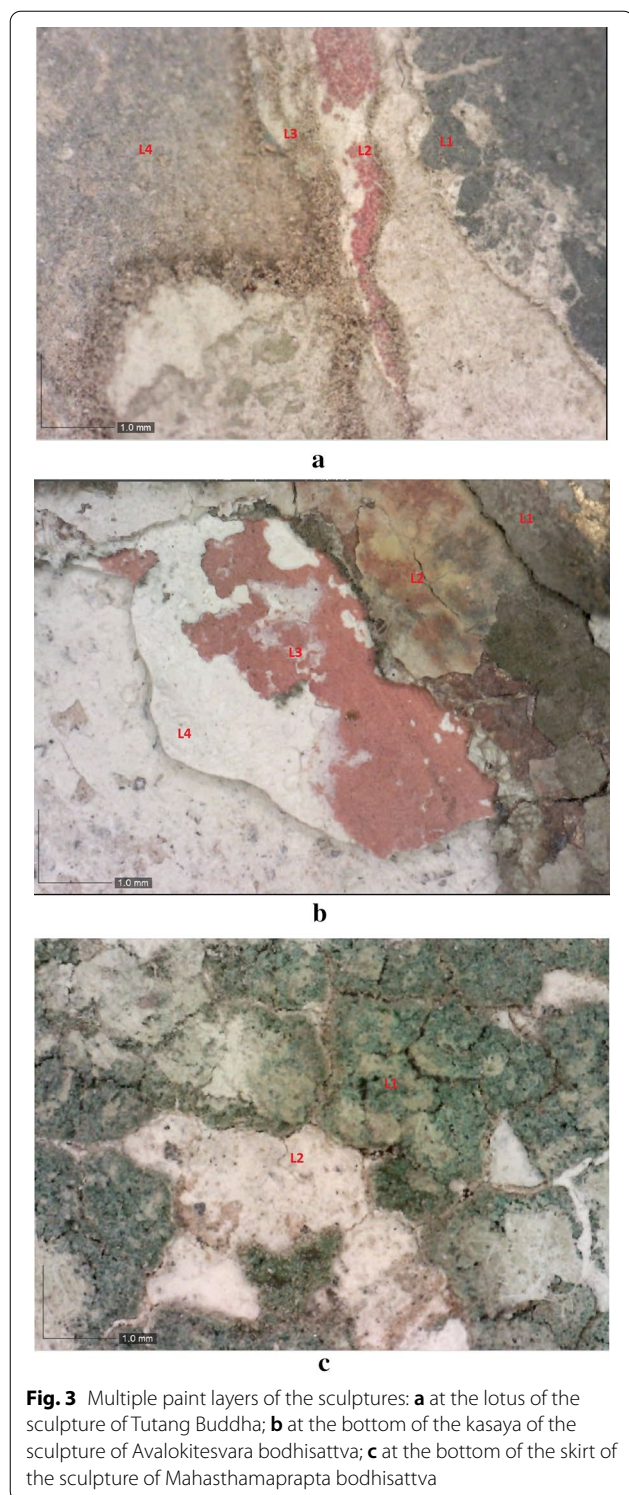
**Results and discussion**

**In-situ observation**

The in-situ microphotographs as shown in Fig. 3, reveal multiple paint layers of the sculptures. The results indicated that the general sequences and combinations of

layers are different for the three sculptures. As seen from Fig. 3a, at least four paint layers were found for the sculpture of Tutang Buddha from top to the bottom, which were: black (L1)–paper–red (L2)–paper–green (L3)–paper–dark green (L4). At the bottom of the kasaya (Fig. 3b), the sequence of the paint layers was gold (L1)–paper–red (L2)–paper–red (L3)–white (L4). In addition, the examination (Fig. 3c) of the sculpture of Mahasthamaprapta bodhisattva demonstrated that the white pigment layer was overlapped by the green pigment layer.

Repainting seriously damaged sculptures was common in ancient China. The ancient Chinese craftsmen usually applied mud and lime to cover the original paint layer and repainted it. Later, mainly in the Ming and Qing dynasties, the processes changed slightly by covering the paint layer with several layers of paper repainted [16]. According to the in-situ observation, at least two layers of paper were found at the three



sculptures with three or four layers of paper in some parts. Meanwhile, the inscriptions proved that the sculptures were restored repeatedly in A.D. 1541 (*the reign of the Jiajing Emperor in the Ming Dynasty*) and A.D. 1739 (*the reign of the Qianlong Emperor in the Qing Dynasty*). Multi-layers paintings were also investigated in the paintings [17] and wooden statues [18]. The result not only helped us to deepen the knowledge of the historical and cultural value but also helped the restorers to determine whether the overlapping layers need to be removed.

#### Analysis of the pigments

The major colours of the sculptures are gold, red, blue, green, white, black, etc. Table 2 shows an overview of the pigments that were identified by SEM–EDS and Micro-Raman spectroscopy (Figs. 4, 5). As shown in Table 1, samples were covered by pollutant minerals (mainly from dust), which caused the detection of elements such as Si, Al, K, Fe in samples [14].

Gilding technique, which uses original materials of gold, silver, copper or tin to the object surface [16, 19–21], has been an ancient technique widely applied in both China and Europe. It has been commonly used in sculptures painting since Song dynasty (A.D. 960–A.D. 1279) [20]. For example, gilding decoration has been applied on the exposed skin and cassock to present the Buddha's magnificence, splendor and solemnity. This technique was also used in decorating the sculptures of Jingyin Temple, as SEM–EDS results (Fig. 4a, f, k) of samples JYS-1-1, JYS-2-2, JYS-3-2 suggested a high level of gold (Au) and further revealed that gold leaf was attached to the surface of the sculptures to form a gorgeous appearance.

SEM–EDS and Micro-Raman were performed on three red pigments. The elements (Fig. 4g) of Hg, S and Pb were found by SEM–EDS in sample JYS-2-3. Different results of the Micro-Raman spectroscopy were obtained at two detection points of red Sample JYS-2-3. At one point, the strong Raman peaks (Fig. 5c) at 252, 286, 342  $\text{cm}^{-1}$ , which corresponded well to characteristic Raman bands of cinnabar (HgS) [22–24]. Moreover, the strong Raman peaks (Fig. 5d) at 160, 225, 313, 475, 546  $\text{cm}^{-1}$  were assigned to minium ( $\text{Pb}_3\text{O}_4$ ). The strong absorption at 546  $\text{cm}^{-1}$  was attributed to the stretching of the Pb–O bond [14, 25, 26]. The result agreed with SEM–EDS analysis and showed the red pigment was a mixture of cinnabar and

**Table 2** The analysis results of major color pigments of the sculptures

Sample	Raman bands (cm <sup>-1</sup> )	Main elements (SEM-EDS)	Pigment
JYS-1-1	/	Au	Gold
JYS-1-2	252, 287, 346	Pb, Hg	Cinnabar + Pb—pigment (red)
JYS-1-3	—	Pb	Pb—pigment (red)
JYS-1-4	152, 278, 1087	Ca	Calcium Carbonate
JYS-1-6	—	—	—
JYS-2-1	—	Pb	Pb—pigment (white)
JYS-2-2	/	Au	Gold
JYS-2-3	252, 286, 342 160,225,313,475,546	Pb, Hg	Cinnabar + Minium
JYS-2-4	137, 174, 247, 400, 543, 766, 836, 944, 1096, 1348, 1425, 1581	Cu	Azurite
JYS-2-5	1051	Pb	Lead White
JYS-3-1	360, 514, 825, 915, 981	Cu	Atacamite
JYS-3-2	/	Au	Gold
JYS-3-3	—	—	—

minium. Using mixed materials of two or more pigments in one color layer is a quite common traditional technique in ancient China [27, 28]. Amount of Hg in sample JYS-1-2 suggests the pigment of cinnabar which has been proved by Micro-Raman. On the other hand, the content of Pb (Fig. 4b) in sample JYS-1-2 may suggest a possibility of the pigment minium. Although the peaks of minium were not detected by Micro-Raman, many investigations [14, 21] of Pb-containing red pigment showed minium was popular used in ancient China. SEM-EDS (Fig. 4c) showed the same result in JYS-1-3.

The blue pigment (JYS-2-4), which was used in decorating the parts of kasaya of the sculpture of Avalokitesvara bodhisattva, was identified as azurite (2CuCO<sub>3</sub>·Cu(OH)<sub>2</sub>). All peaks (Fig. 5e) between 100 and 1600 cm<sup>-1</sup> (137, 174, 247, 400, 543, 766, 836, 944, 1096, 1348, 1425 and 1581 cm<sup>-1</sup>) were diagnostic Raman peaks assigned to azurite [29]. The main element (Fig. 4h) of the sample was Cu detected by SEM-EDS. It is well known that azurite was a most important blue mineral pigment both in ancient China [30] and in the European Middle Ages paintings [31]. The skirt and streamer of the sculpture of Mahasthamaprapta bodhisattva were painted with green pigment and gold which formed the brilliant colors and exquisite patterns. The green pigment (JYS-3-1) was identified as atacamite (Cu<sub>2</sub>Cl(OH)<sub>3</sub>). SEM-EDS analysis (Fig. 4j) reported relatively high level of Cu. Micro-Raman study (Fig. 5g) of the sample showed peaks at

360, 514, 825, 915, 981 cm<sup>-1</sup>, which were assigned to atacamite [32, 33].

Moreover, three white pigments were identified. Sample JYS-1-4 was calcium carbonate (CaCO<sub>3</sub>) [34], identified by its characteristic Raman band at (Fig. 5b) at 152, 278, 1087 cm<sup>-1</sup> and large amount of Ca (Fig. 4d). Calcium carbonate has been used to paint white for quite a long time and was reported to be used in the art and archaeological objects, such as the mural painting [35, 36], architecture, et al. More interestingly, the main chemical constituent (Fig. 4i) of the white pigments of JYS-2-5 is Pb. The Raman band (Fig. 5f) registered at 1051 cm<sup>-1</sup> is attributed to lead white (2PbCO<sub>3</sub>·Pb(OH)<sub>2</sub>) [12]. Lead white, based on basic lead carbonate, was known since ancient times due to its high covering power, and was the most commonly used white pigment until the nineteenth century [29]. Although Micro-Raman spectroscopy does not provide the peaks of lead white, given the white color and large amount of Pb (Fig. 4e), it would be reasonable to assume that the white pigment of sample JYS-2-1 is lead white, as many investigations [33, 37] have indicated that lead white was popular used in Chinese history. The result overall indicated that the sculpture of Avalokitesvara bodhisattva was decorated by the white pigment of lead white.

Although Raman spectrometer is a helpful technique in the identification of the pigments, it should be mentioned that there are still limitations, such as certain pigments cannot be identified due to the strong

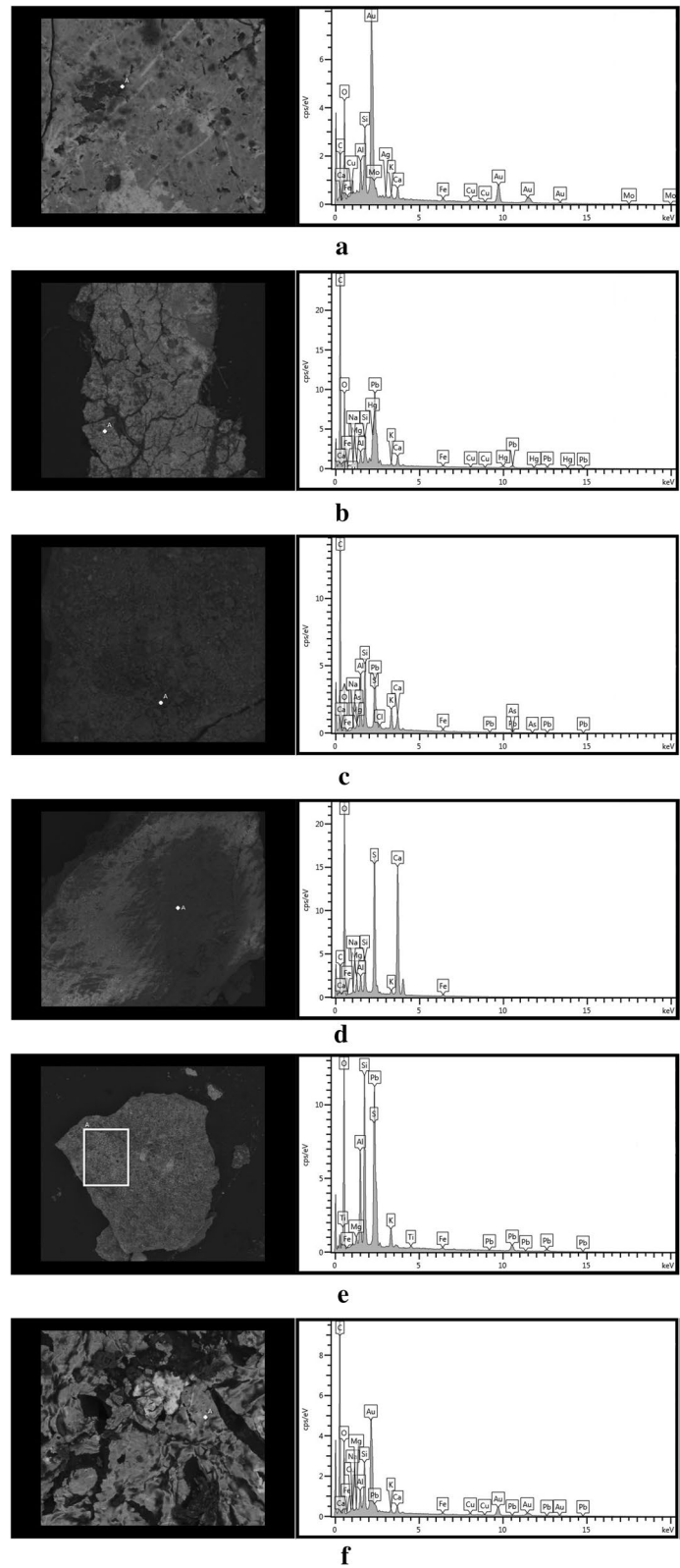


**Fig. 4** SEM/EDS results of the samples: **a** JYS-1-1; **b** JYS-1-2; **c** JYS-1-3; **d** JYS-1-4; **e** JYS-2-1; **f** JYS-2-2; **g** JYS-2-3; **h** JYS-2-4; **i** JYS-2-5; **j** JYS-3-1; **k** JYS-3-2

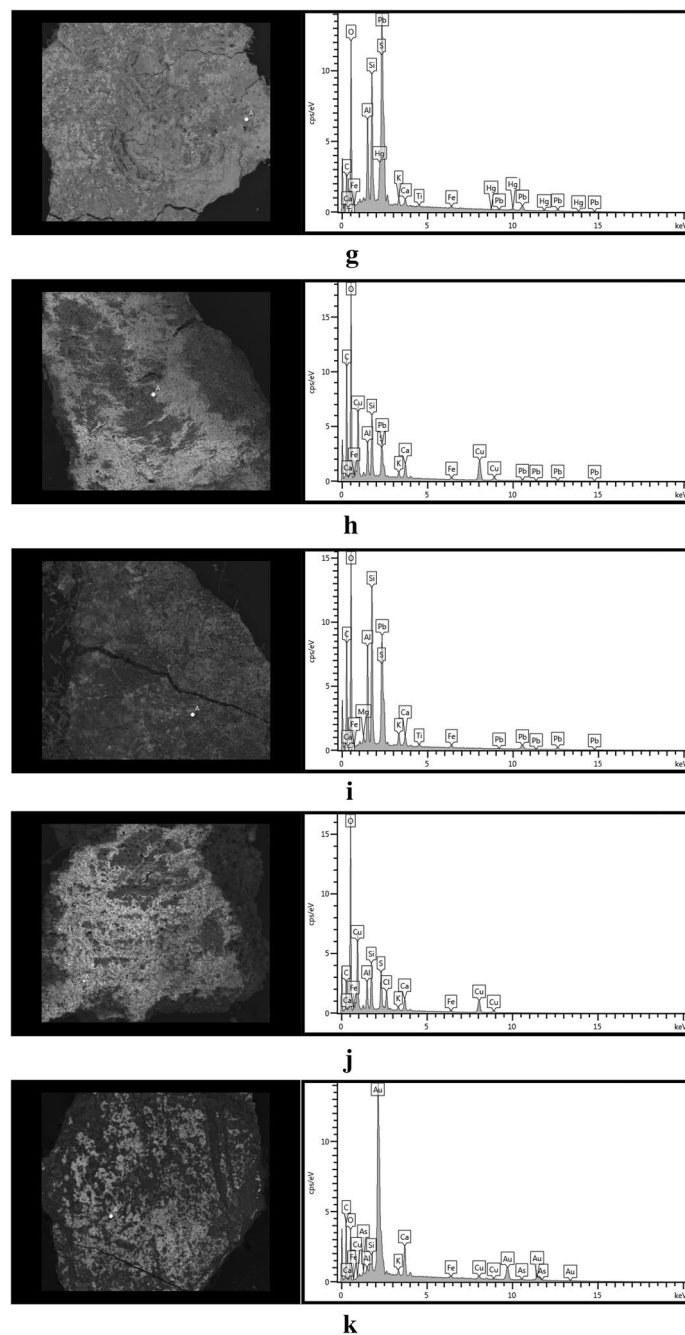
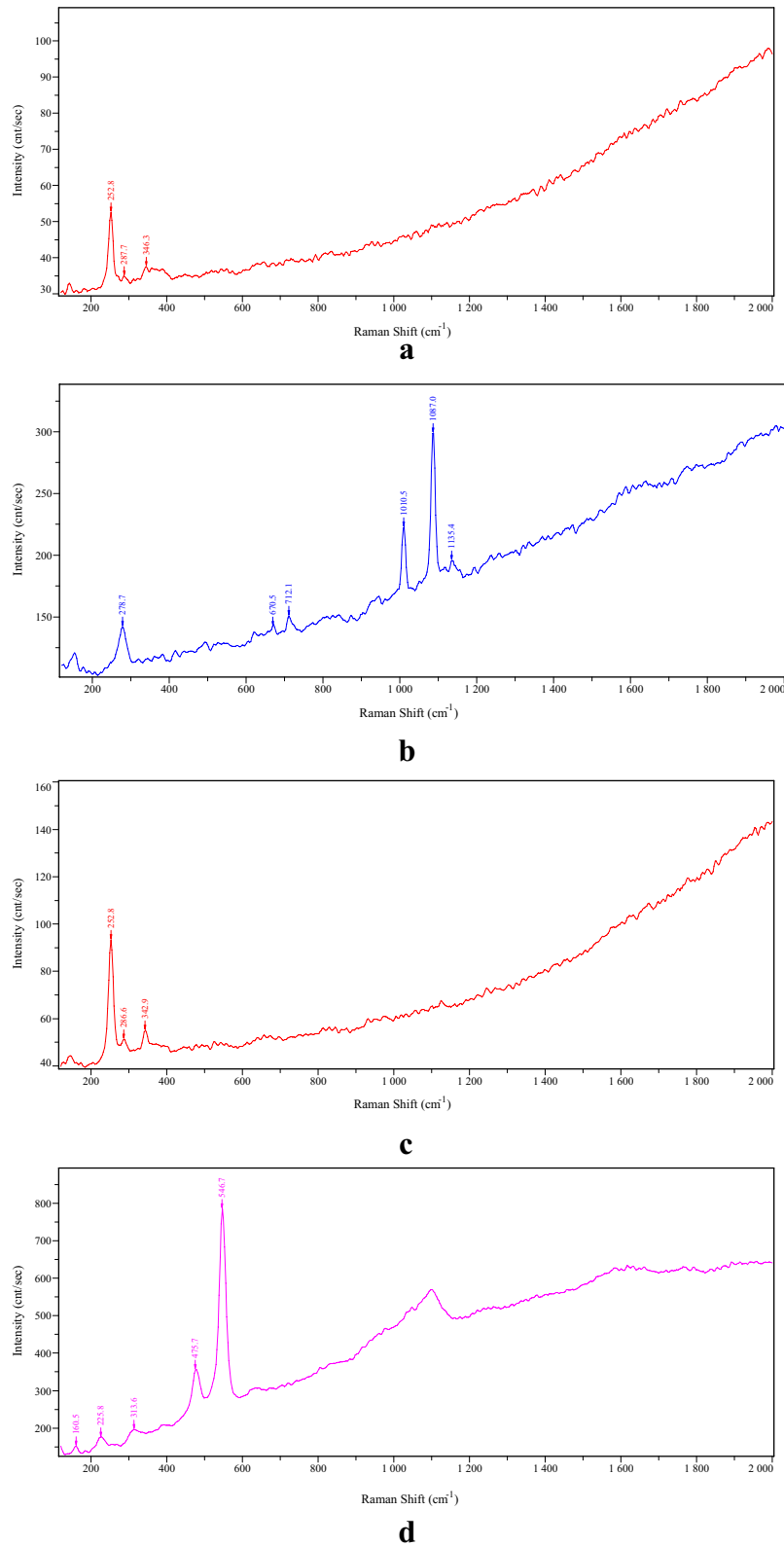


Fig. 4 continued

fluorescence arising from the binding agent [38], the color and the compositions of the pigments were damaged due to the ageing, smoke damage and pollution [39], etc. For black pigment [40, 41], the Raman band position and intensity depend on the carbon type, on

the amount of disorder, on the orientation of the crystal with respect to the laser and on the measurement conditions.

Unfortunately, mainly due to the poor conservation or other reasons, Micro-Raman spectroscopy analysis failed



**Fig. 5** Raman spectrum of samples: **a** JYS-1-2; **b** JYS-1-4; **c** JYS-2-3-1; **d** JYS-2-3-2; **e** JYS-2-4; **f** JYS-2-5; **g** JYS-3-1

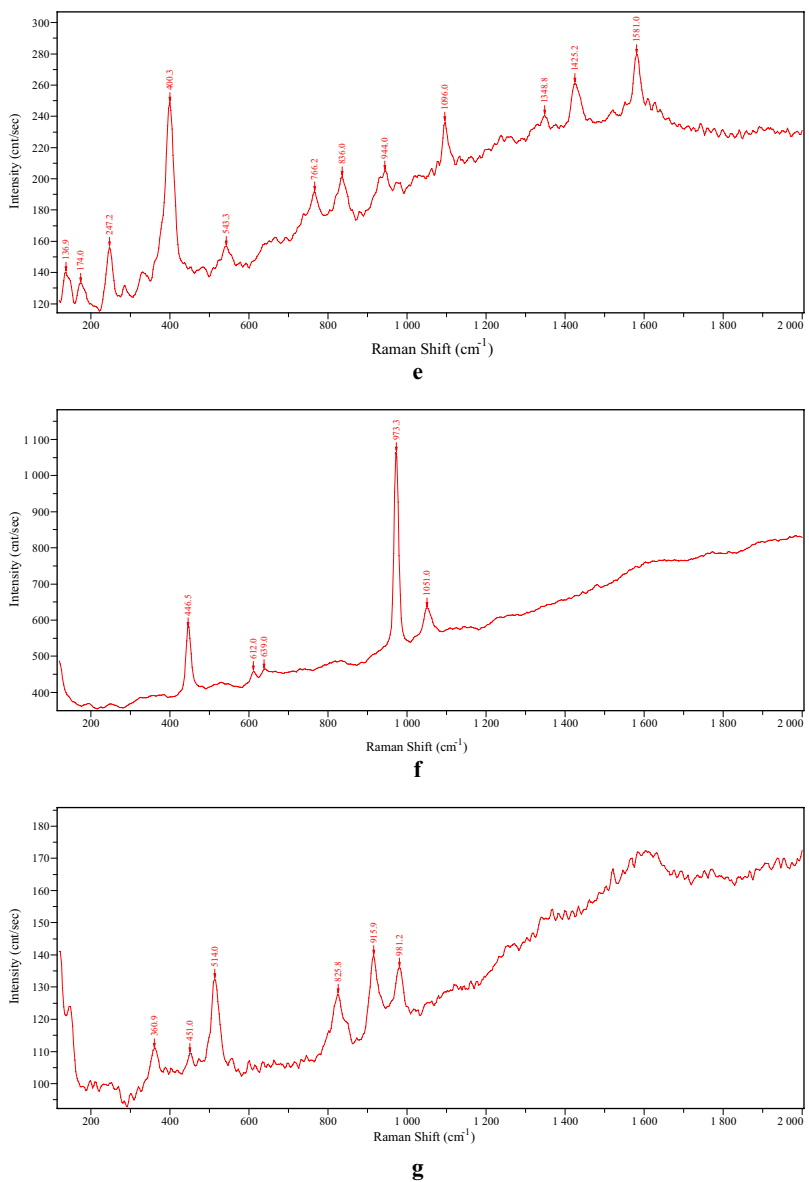
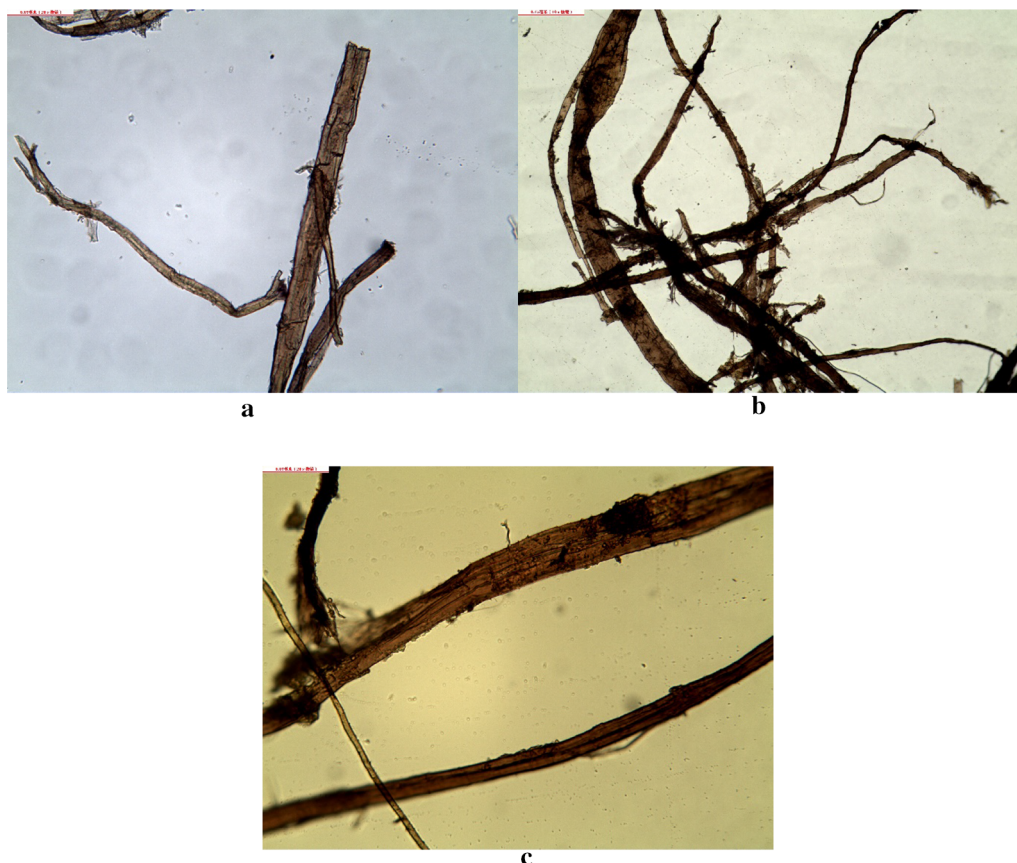


Fig. 5 continued

to identify black pigments. A mass of literatures [40, 42] show that carbon-based pigments, of mineral, vegetable or animal origin, composed ideally of pure carbon, have been identified in archaeological artifacts [43, 44], rock art [45, 46], easel and wall paintings [47], and sculptures [41]. Especially, the black pigments were determined to carbon-based black pigment in the painting [30, 48, 49] and sculptures [7, 50] which is the same period with the Jingyin Temple. Based on the previous studies, it is

interesting to speculate that carbon-based black pigment may also be used in the sculptures at Jingyin Temple. While the case could not be eliminated that the black pigments may be the organic compound due to the accumulation of long time smudging by folk burning incense in the devotional practice or the soot deposition resulting from burning bonfires [28]. Hopefully, further analytical methods could be used to provide more reliable evidence for the black pigment in the future.



**Fig. 6** Morphology of paper fibers: **a** JYS-1-1; **b** JYS-2-4; **c** JYS-3-1

#### **Fiber identification of paper**

Herzberg stain is usually used to distinguish fiber sources, because different fibers sources are dyed in different colors by the iodide/iodine mixed with zinc chloride solution [12]. After dyeing, the three paper fibers were shown as reddish brown in Fig. 6a–c. The thickness of the fibers are different, in the range of 12–60  $\mu\text{m}$ . There are numerous longitudinal stripes and transversal striations on the fiber walls. By comparing stained fibers with those most commonly used in Oriental papermaking, such as bast fibers (hemp, flex, ramie, paper mulberry, etc.), bamboos, and grass fibers (wheat and rice straws), it is indicated that the fiber sources of the three samples are ramie [51]. It is well known that ramie has its origin in China. Documental evidences show Tsai-lun invented a new process of paper-making, and ramie has been used as one of the materials in Eastern Han dynasty [15] till now.

#### **Phase identification of Clay minerals**

Only samples of fine clay layer were taken for test due to the technical limitation. XRD patterns shown in Fig. 7 suggested that quartz ( $\text{SiO}_2$ ) [52] and calcite ( $\text{CaCO}_3$ ) [53] were the primary crystalline phases in the fine clay layers and the soil from the hillside close to Jingyin Temple. The presence of minor albite ( $\text{Na(AlSi}_3\text{O}_8)$ ) and gypsum ( $\text{Ca(SO}_4\text{)(H}_2\text{O)}_2$ ) in both JYS-2-6 and JYS-3-4 indicated they were applied simultaneously. XRD analyses revealed albite ( $\text{Na(AlSi}_3\text{O}_8)$ ) was the minor component of JYS-1-5. The granulometric results of JYS-4, JYS-1-5, JYS-2-6, JYS-3-4 in Table 3 showed the particle sizes were mainly in the range of 0.0002–0.20 mm. The component particles of the samples were predominantly between 0.075 mm and 0.01 mm, with the content of coarse powder particle over 50%. It is also found that the particle size distributions, clay mineral compositions of



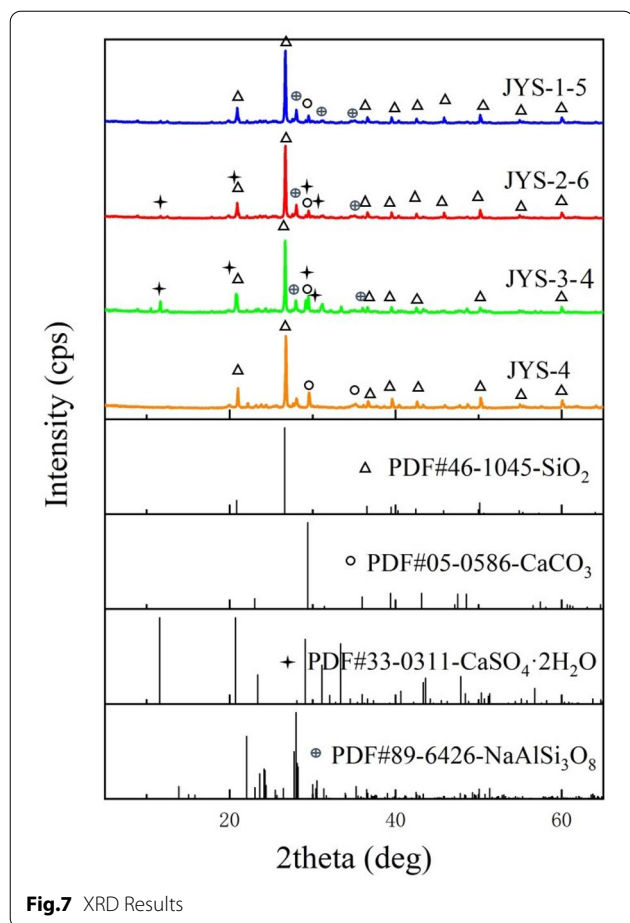


Fig.7 XRD Results

fine clay layer and the color of the three sculptures were similar with those collected from the Juewei Mountain. Relevant studies suggested that the craftsmen made clay sculptures by collecting the raw materials from local area [54, 55]. Based on the previous research and the analytical results, the sources of the material remain uncertain, but the result is important for working out the restoration scheme and filtering the restoration materials.

**Conclusion**

These well painted sculptures of Jingyin Temple boast high standard and exquisite craft. Unfortunately, owing to the deterioration factors, the sculptures were damaged severely. Therefore, these cultural relics need urgent protection and restoration.

However, the materials and crafts used in making the sculptures of Jingyin Temple have been barely studied so far. To fill the gap, in this study, several scientific techniques were used to investigate the technology and materials of the sculptures making, with very interesting and unique results: a mixture of cinnabar and minium, chlorite, azurite, calcium carbonate were identified as red pigments, green pigment, blue pigment, white pigment, respectively; gold foils were used to paint the outer surfaces of the sculptures; the sculptures were redrawn; the particle size distributions, clay mineral compositions of fine clay layer of the three sculptures were similar with those collected from the Juewei Mountain.

The results provided scientific evidence in establishing applicable conservation schemes and selecting the applicable restoration materials. Furthermore, suggestions on

**Table 3 Particle size distribution of the fine clay layer**

Particle size(mm)						
Ratio (%)	Coarse sand	Medium sand	Fine sand	Coarse powder particle	Fine powder particle	Clay particle
Sample no	0.5 < d ≤ 2	0.25 < d ≤ 0.5	0.075 < d ≤ 0.25	0.01 < d ≤ 0.075	0.005 < d ≤ 0.01	d ≤ 0.005
JYS-1-5	/	/	8.45	60.24	15.29	16.02
JYS-2-6	/	/	8.67	62.21	14.82	14.30
JYS-3-4	/	/	7.89	61.45	15.63	15.03
JYS-4	/	/	6.17	58.03	16.56	19.24

the preservation of these cultural relics were discussed in this research.

#### Abbreviations

SEM–EDS: Scanning electron microscopy in combination with energy dispersive X-ray analysis; XRD: X-ray diffraction; OM: Optical microscopy; Raman: Micro-Raman spectroscopy combined with optical microscopy.

#### Acknowledgements

The authors are grateful to Meifeng Shi, Shanxi Museum for Raman and SEM investigation. Thanks for Wenwen Cai, Beijing Guowenyan Conservation and Development of Cultural Heritage Co., Ltd. for providing the photographs of In-situ observation.

#### Authors' contributions

XB designed the experiment; prepared the samples; performed the data analysis; wrote the manuscript. CJ and ZC provided the samples and interpreted the information of statues restoration; helped for writing and revised the article. YG wrote and revised the article. HC provided the photographs of the sculptures; revised the article. JW participated in completing part of the analysis. All authors read and approved the final manuscript.

#### Funding

This work was financially supported by MOE (Ministry of Education in China) Project of Humanities and Social Sciences (Grant No. 16YJCZH001).

#### Availability of data and materials

All data generated or analyzed during this study are included in this published article.

#### Competing interests

The authors declare that they have no competing interests.

#### Author details

<sup>1</sup> Department of Cultural Heritage, Taiyuan University of Technology, Taiyuan 030024, China. <sup>2</sup> Cultural Relics Conservation Department of Juewei Mountain, Taiyuan 030051, China. <sup>3</sup> Department for the History of Science and Scientific Archaeology, University of Science and Technology of China, Hefei 230026, China. <sup>4</sup> Shanxi Cultural Relic and Natural History Group Co Ltd, Taiyuan 030013, China.

Received: 30 March 2020 Accepted: 6 December 2020

Published online: 05 January 2021

#### References

- Liu ZM. Compiling Record of Stone Carvings in Shanxi Province Vol. Jiancaoping District. Taiyuan: Sanjin Press; 2012. p. 35–36 (In Chinese).
- Fang SK. Cultural Resources in Taiyuan. Taiyuan: Shanxi People's Publishing House; 2009. p. 68–70 (In Chinese).
- Academy D. Dunhuang grottoes art. Shanghai: Tongji University Press; 2016. p. 48–51 (In Chinese).
- Cao CP. Traditional Architecture of South Area of Fujian Province. Xiamen: Xiamen University Press; 2006. p. 240 (In Chinese).
- Li LS, Du JG, Liu HL, Chen RH, Liu T. Dynamic characteristics and seismic responses of painted sculptures of Dunhuang Mogao Grottoes. *J Cult Herit*. 2016;22:1040–8. <https://doi.org/10.1016/j.culher.2016.07.003>.
- Egel E, Simon S. Investigation of the painting materials in Zhongshan Grottoes (Shaanxi, China). *Herit Sci*. 2013. <https://doi.org/10.1186/2050-7445-1-29>.
- Ma YY, Zhang JH, Hu DB. Scientific analysis of a Ming Dynasty polychrome star sculpture from Shanxi Art Museum, Taiyuan. *China Sci Conserv Archaeol*. 2015;27(4):50–60 (In Chinese).
- Hernanz A, Iriarte M, Bueno-Ramirez P, De Balbín-Behrmann R, Gavira-Vallejo J, Calderón-Saturio D, Laporte L, Barroso-Bermejo R, Gouezin P, Maroto-Valiente A, Salanova L, Benetau-Douillard G, Mens E. Raman microscopy of prehistoric paintings in French megalithic monuments. *J Raman Spectrosc*. 2016;47(5):571–8. <https://doi.org/10.1002/jrs.4852>.
- Gong YX, Qiao CQ, Zhong BC, Zhong JR, Gong DC. Analysis and characterization of materials used in heritage theatrical figurines. *Herit Sci*. 2020;8(1):1–18. <https://doi.org/10.1186/s40494-020-0358-7>.
- Svarcova S, Bezdicka P, Hradil D, Hradilov J, Zizak I. Clay pigment structure characterisation as a guide for provenance determination—a comparison between laboratory powder micro-XRD and synchrotron radiation XRD. *Anal Bioanal Chem*. 2011;399(1):331–6. <https://doi.org/10.1007/s00216-010-4382-4>.
- Huang F. Research on the Conservation of Color-painted Sculptures of the Tang Dynasty of Foguang Temple in Wutai. M.A. dissertation: University of Science and Technology of China 2014 (In Chinese).
- Li T, Ji JX, Zhou Z, Shi JL. A multi-analytical approach to investigate date-unknown paintings of Chinese Taoist priests. *Archaeol Anthropol Sci*. 2017;9(3):395–404. <https://doi.org/10.1007/s12520-015-0293-9>.
- ICOMOS China. Principles for the Conservation of Heritage Sites in China. Beijing: Cultural Relics Press; 2015. p. 10–15 (In Chinese).
- Liu L, Gong DC, Yao ZQ, Xu LJ, Zhu ZY, Eckfeld T. Characterization of a Mahamayuri Vidyarajini Sutra excavated in Lu'an. *China Herit Sci*. 2019;7(1):1–9. <https://doi.org/10.1186/s40494-019-0320-8>.
- Wang JH. Papermaking raw materials of China An atlas of micrographs and the characteristics of fibers. Beijing: China Light Industry Press; 1999. p. 163 170 (In Chinese).
- Chen J. The technique of making the Buddhist statues in China. Shanghai: Tongji University Press; 2011. p. 10–30 (In Chinese).
- Henderson EJ, Helwig K, Read S, Rosendahl SM. Infrared chemical mapping of degradation products in cross-sections from paintings and painted objects. *Herit Sci*. 2019. <https://doi.org/10.1186/s40494-019-0313-7>.
- Fermo P, Mearini A, Bonomi R, Arrighetti E, Comite V. An integrated analytical approach for the characterization of repainted wooden statues dated to the fifteenth century. *Microchem J*. 2020;157:1–13. <https://doi.org/10.1016/j.microc.2020.105072>.
- Crina Anca Sandu I, Helena de Sá M, Costa Pereira M. Ancient “gilded” art objects from European cultural heritage: a review on different scales of characterization. *Surf Interface Anal*. 2011;43:1134–51. <https://doi.org/10.1002/sia.3740>.
- Wang N, He L, Egel E, Simon S, Rong B. Complementary analytical methods in identifying gilding and painting techniques of ancient clay-based polychromic sculptures. *Microchim J*. 2014;114:125–40. <https://doi.org/10.1016/j.microc.2013.12.011>.
- Zhou ZB, Shen L, Wang N, Ren XX, Yang J, Shi YC, Zhang H. Identification of organic materials used in gilding technique in wall paintings of Kizil Grottoes. *Chem Sel*. 2020;5(2):818–22. <https://doi.org/10.1002/slct.201903688>.
- Gard FS, Santos DM, Daizo MB, Freire E, Reinoso M, Halac EB. Pigments analysis of an Egyptian cartonnage by means of XPS and Raman spectroscopy. *Appl Phys A-Mater*. 2020;126(3):1–12. <https://doi.org/10.1007/s00339-020-3386-y>.
- Arriaza B, Ogalde JP, Campos M, Paipa C, Leyton P, Lara N. Toxic Pigment in a Capacocho Burial: Instrumental Identification of Cinnabar in Inca Human Remains from Iquique Chile. *Archaeometry*. 2018;60(6):1324–33. <https://doi.org/10.1111/arc.12392>.
- Liu ZF, Zhang H, Zhou WH, Hao SC, Zhou Z, Qi XK, Shi JL. Pigment identification on an undated Chinese painting by non-destructive analysis. *Vib Spectrosc*. 2019;101:28–33. <https://doi.org/10.1016/j.vibspec.2018.08.009>.
- Stanzani E, Bersani D, Lottici PP, Colomban P. Analysis of artist's palette on a 16th century wood panel painting by portable and laboratory Raman instruments. *Vib Spectrosc*. 2016;85:62–70. <https://doi.org/10.1016/j.vibspec.2016.03.027>.
- Dominguez-Vidal A, De la Torre-López MJ, Campos-Suñol MJ, Rubio-Domene R, Ayora-Canada MJ. Decorated plasterwork in the Alhambra investigated by Raman spectroscopy: comparative field and laboratory study. *J Raman Spectrosc*. 2014;45(1):1006–12. <https://doi.org/10.1002/jrs.4439>.
- Chen XL, Xia Y, Ma YR, Lei Y. Three fabricated pigments (Han purple, indigo and emerald green) in ancient Chinese artifacts studied by Raman microscopy, energy-dispersive X-ray spectrometry and polarized light microscopy. *J Raman Spectrosc*. 2008;38(10):1274–9. <https://doi.org/10.1002/jrs.1766>.
- He L, Wang N, Zhao X, Zhou T, Xia Y, Liang JY, Rong B. Polychromic structures and pigments in Guangyuan Thousand-Buddha Grotto of the

- Tang Dynasty (China). *J Archaeol Sci.* 2012;39(6):1809–20. <https://doi.org/10.1016/j.jas.2012.01.022>.
29. Gutman M, Lesar-Kikelj M, Mladenovic A, Cobal-Sedmak V, Kriznar A, Kramar SD. Raman microspectroscopic analysis of pigments of the Gothic wall painting from the Dominican Monastery in Ptuj (Slovenia). *J Raman Spectrosc.* 2014;45:1103–9. <https://doi.org/10.1002/jrs.4628>.
  30. Chen EX, Zhang BJ, Zhao F, Wang C. Pigments and binding media of polychrome relics from the central hall of Longju temple in Sichuan. *China Herit Sci.* 2019. <https://doi.org/10.1186/s40494-019-0289-3>.
  31. Lluveras A, Boulerand S, Andreotti A, Vendrell-Saz M. Degradation of azurite in mural paintings: distribution of copper carbonate, chlorides and oxalates by SRFTIR. *Appl Phys A-Mater.* 2010;99(2):363–75. <https://doi.org/10.1007/s00339-010-5673-5>.
  32. Holakooei P, de Lapérouse JF, Rugiadi M, Caro F. Early Islamic pigments at Nishapur, north-eastern Iran: studies on the painted fragments preserved at The Metropolitan Museum of Art. *Archaeol Anthropol Sci.* 2018;10(1):175–95. <https://doi.org/10.1007/s12520-016-0347-7>.
  33. Hu KJ, Bai CB, Ma LY, Bai K, Liu DB, Fan BB. A study on the painting techniques and materials of the murals in the Five Northern Provinces' Assembly Hall, Ziyang China. *Herit Sci.* 2013. <https://doi.org/10.1186/2050-7445-1-18>.
  34. Hussein AM, Madkour FS, Afifi HM, Abdel-Ghani M, Elfatah MA. Comprehensive study of an ancient Egyptian foot case cartonnage using Raman, ESEM-EDS XRD and FTIR. *Vib Spectrosc.* 2020. <https://doi.org/10.1016/j.vibspec.2019.102987>.
  35. Debastiani R, Simon R, Goettlicher J, Heissler S, Steininger R, Batchelor D, Fiederle M, Baumbach T. Identification of green pigments from fragments of Roman mural paintings of three Roman sites from north of Germania Superior. *Appl Phys A-Mater.* 2016;122(10):1–12. <https://doi.org/10.1007/s00339-016-0400-5>.
  36. Kigawaa R, Sanoa C, Nishijima M, Tazatob N, Kiyunab T, Hayakawaa N, Kawanobea W, Udagawac S, Tateishic T, Sugiyamab J. Investigation of acetic acid bacteria isolated from the Kitora tumulus in Japan and their involvement in the deterioration of the plaster of the mural paintings. *Stud Conserv.* 2013;58(1):30–40. <https://doi.org/10.2307/42751795>.
  37. Li T, Liu C, Wang DM. Applying micro-computed tomography (micro-CT) and Raman spectroscopy for non-invasive characterization of coating and coating pigments on ancient Chinese papers. *Herit Sci.* 2020;8(1):1–16. <https://doi.org/10.1186/s40494-020-00366-3>.
  38. Lauwers D, Cattersel V, Vandamme L, Van-Eester A, De-Langhe K, Moens L, Vandenabeele P. Pigment identification of an illuminated mediaeval manuscript De Civitate Dei by means of a portable Raman equipment. *J Raman Spectrosc.* 2014;45:1266–71. <https://doi.org/10.1002/jrs.4500>.
  39. Yi L, Wang FP, Fu XY, Sun ZJ, Xu YQ. Analysis of the pigments for smoked mural by confocal micro-Raman spectroscopy. *J Raman Spectrosc.* 2017;48(11):1479–86. <https://doi.org/10.1002/jrs.5158>.
  40. Coccato A, Jehlicka J, Moens L, Vandenabeele P. Raman spectroscopy for the investigation of carbon-based black pigments. *J Raman Spectrosc.* 2015;46(10):1003–15. <https://doi.org/10.1002/jrs.4715>.
  41. Tomasini EP, Gómez B, Halac EB, Reinoso M, Di Liscia EJ, Siracusano G, Maier MS. Identification of carbon-based black pigments in four South American polychrome wooden sculptures by Raman microscopy. *Herit Sci.* 2015. <https://doi.org/10.1186/s40494-015-0049-y>.
  42. Winter J. The characterization of pigments based on carbon. *Stud Conserv.* 1983;28(2):49–66. <https://doi.org/10.1179/sic.1983.28.2.49>.
  43. Aldazabal V, Reinoso M, Custo G, Cerchetti L, Halac EB, Polla G, Freire E. Characterization of Natural Pigments from the Archaeological Context of Triful Lake (Neuquén, Argentina). *Lat Am Antiq.* 2019;30(1):127–41. <https://doi.org/10.1017/laq.2018.75>.
  44. Vettori S, Bracci S, Cantisani E, Conti C, Ricci M, Caggia MP. Archaeometric and archaeological study of painted plaster from the Church of St. Philip in Hierapolis of Phrygia (Turkey). *J Archaeol Sci.* 2019;24:869–78. <https://doi.org/10.1016/j.jasrep.2019.03.008>.
  45. Lopez-Montalvo E, Villaverde V, Roldan C, Murcia S, Badal E. An approximation to the study of black pigments in Cova Remigia (Castellón, Spain). Technical and cultural assessments of the use of carbon-based black pigments in Spanish Levantine Rock Art. *J Archaeol Sci.* 2014;52:535–45. <https://doi.org/10.1016/j.jas.2014.09.017>.
  46. Rosina P, Oosterbeek L, Martins CP, Gomes H. Dating and Raman spectroscopy of rock art paintings in Ebo. *Angola Azania.* 2018;53(1):83–97. <https://doi.org/10.1080/0067270X.2018.1423758>.
  47. Tomasini E, Siracusano G, Maier MS. Spectroscopic, morphological and chemical characterization of historic pigments based on carbon. Paths for the identification of an artistic pigment. *Microchem J.* 2012;102:28–37. <https://doi.org/10.1016/j.microc.2011.11.005>.
  48. Xu LN, Guo H. Research on materials and technology of shoufeng temple mural painting in Shaanxi Province. *Res Herit Pres.* 2018;3(8):12–5 (In Chinese).
  49. Shen A, Wang XH, Xie W, Shen J, Li HY, Liu ZA, Hu JM. Pigment identification of colored drawings from Wuying Hall of the Imperial Palace by micro-Raman spectroscopy and energy dispersive X-ray spectroscopy. *J Raman Spectrosc.* 2007;37(1):230–4. <https://doi.org/10.1002/jrs.1435>.
  50. Hui R, Feng YY, Lu ZY, Fu QL, Wang Z. Scientific analysis of sculptures in Wanfo Pavilion of Baoen Temple, Pingwu. *Sichuan Province Archaeol Cult Relics.* 2018;3:118–25 (In Chinese).
  51. Shi JL, Li T. Technical investigation of 15th and 19th century Chinese paper currencies Fiber use and pigment identification. *J Raman Spectrosc.* 2013;44(6):892–8. <https://doi.org/10.1002/jrs.4297>.
  52. Salama KK, Ali MF, El-Sheikh SM. Examination and analysis of an Egyptian Coptic Fresco from Saint Jeremiah Monastery. *J Sci Arts.* 2019;19(1):153–62.
  53. Garofano I, Perez-Rodriguez JL, Robador MD, Duran A. An innovative combination of non-invasive UV-Visible-FORS, XRD and XRF techniques to study Roman wall paintings from Seville. *Spain J Cult Herit.* 2016;22:1028–39. <https://doi.org/10.1016/j.culher.2016.07.002>.
  54. Fan J. The Study of the material properties and restorative material of clay sculpture at Shuiluan. *Archaeol Cult Relics.* 1994;6:30–41 (In Chinese).
  55. Li YF, Wang XD, Zhao LY, Fan YQ, Fu P, Li B, Yang T. The study of the material and craft used in making painted sculpture at the Houtu Temple of Jiexiu. *Shanxi Dunhuang Res.* 2007;5:54–8 (In Chinese).

## Publisher's Note

Springer Nature remains neutral with regard to jurisdictional claims in published maps and institutional affiliations.

Submit your manuscript to a SpringerOpen® journal and benefit from:

- Convenient online submission
- Rigorous peer review
- Open access: articles freely available online
- High visibility within the field
- Retaining the copyright to your article

Submit your next manuscript at ► [springeropen.com](https://www.springeropen.com)